Molecular Recognition at Methyl Methacrylate/n-Butyl Acrylate (MMA/nBA) Monomer Unit Boundaries of Phospholipids at p-MMA/nBA Copolymer Surfaces

4 AUTHORS, INCLUDING:

Yinghong Sheng
Florida Gulf Coast University
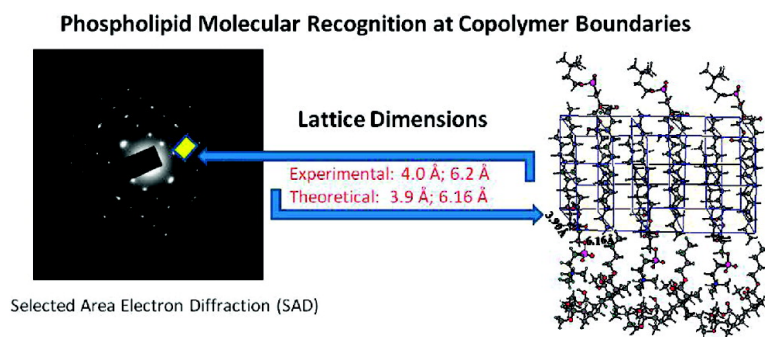35 PUBLICATIONS 415 CITATIONS

SEE PROFILE

Molecular Recognition at Methyl Methacrylate/n-Butyl Acrylate (MMA/nBA) Monomer Unit Boundaries of Phospholipids at p-MMA/nBA Copolymer Surfaces

Min Yu, Marek W. Urban, Yinghong Sheng, and Jerzy Leszczynski

Phospholipid Molecular Recognition at Copolymer Boundaries

Lattice Dimensions

Experimental: 4.0 Å; 6.2 Å
Theoretical: 3.9 Å; 6.16 Å

Selected Area Electron Diffraction (SAD)

More About This Article

Additional resources and features associated with this article are available within the HTML version:

- Supporting Information
- Access to high resolution figures
- Links to articles and content related to this article
- Copyright permission to reproduce figures and/or text from this article

View the Full Text HTML

Molecular Recognition at Methyl Methacrylate/n-Butyl Acrylate (MMA/nBA) Monomer Unit Boundaries of Phospholipids at p-MMA/nBA Copolymer Surfaces

Min Yu,[†] Marek W. Urban,[*,†] Yinghong Sheng,[‡,§] and Jerzy Leszczynski[*,‡]

School of Polymers and High Performance Materials, Shelby F. Thames Polymer Science Research Center, The University of Southern Mississippi, Hattiesburg, Mississippi 39406, and The Computational Center for Molecular Structure and Interactions, Department of Chemistry, Jackson State University, Jackson, Mississippi 39217

Lipid structural features and their interactions with proteins provide a useful vehicle for further advances in membrane proteins research. To mimic one of potential lipid−protein interactions we synthesized poly(methyl methacrylate/*n*-butyl acrylate) (p-MMA/nBA) colloidal particles that were stabilized by phospholipid (PLs). Upon the particle coalescence, PL stratification resulted in the formation of surface localized ionic clusters (SLICs). These entities are capable of recognizing MMA/nBA monomer interfaces along the p-MMA/nBA copolymer backbone and form crystalline SLICs at the monomer interface. By utilizing attenuated total reflectance Fourier transform infrared (ATR FT-IR) spectroscopy and selected area electron diffraction (SAD) combined with ab initio calculations, studies were conducted that identified the origin of SLICs as well as their structural features formed on the surface of p-MMA/nBA copolymer films stabilized by 1,2-dilauroyl-*sn*-glycero-3-phosphocholine (DLPC) PL. Specific entities responsible for SLIC formation are selective noncovalent bonds of anionic phosphate and cationic quaternary ammonium segments of DLPC that interact with two neighboring carbonyl groups of nBA and MMA monomers of the p-MMA/nBA polymer backbone. To the best of our knowledge this is the first example of molecular recognition facilitated by coalescence of copolymer colloidal particles and the ability of PLs to form SLICs at the boundaries of the neighboring MMA and nBA monomer units of the p-MMA/nBA chain. The dominating noncovalent bonds responsible for the molecular recognition is a combination of H-bonding and electrostatic interactions.

Introduction

Noncovalent interactions play an important role in biological systems and there are numerous examples of molecular recognition at interfaces ranging from crystal interfaces[1,2] to base-pairing,[3] peptide and DNA recognition,[4,5] and sensing.[6] Mother Nature has mastered these processes and, with just a few building blocks, is capable of signaling and recognizing subtle changes through manipulations of noncovalent, typically weak hydrogen bonding interactions. One biopolymer that is capable of encoding genetic data is DNA, and among other functions its sequence determines the type of organism or disease susceptibility, but its critical feature is the ability to precisely encode a specific protein sequence.[5] The key component in these processes is molecular recognition and the ability of selective binding to specific molecular segments. Another example is proper matching between hydrophobic components of proteins with more flexible lipid molecules which tend to surround the former by matching sizes and shapes. Due to protein rigidity and relatively flexible lipids, the conditions of hydrophobic matching can by accomplished by

structural rearrangements of lipid rafts. The main question in these and other studies is what chemical entities are responsible for structural matching and molecular recognition? Thus, one of the challenges, and at the same time opportunity for creating materials with supramolecular structures with signaling characteristics, is their ability of recognizing other species not necessarily via covalent bond formation, but other typically weaker, but orchestrated interactions.

In view of these considerations, we recently explored film formation processes of colloidal particles that were deliberately stabilized by biologically active and surface stabilizing phospholipids (PL).[7−10] These studies showed that colloid particle morphologies play an essential role in coalescence and exhibit particular influence on interfacial regions near the film−air (F-A) and film−substrate (F-S) interfaces. One of the outcomes of these studies was the formation of surface localized rafts that exhibit stimuli-responsive characteristics controlled by colloidal particle-phospholipid interactions as well as pH and temperature. These surface entities resemble the natural phenomena of membrane lipid rafts and may have significant implications on further advances leading to understanding mechanistic aspects of cell−cell signaling, endocytosis, and raft−raft cross-talk.[11,12] During the course of these studies unique structural features were identified which were inherently associated with particle coalescence and copolymer composition, as well as structural

---
* To whom correspondence should be addressed. E-mail: marek.urban@usm.edu (M.W.U.).

† The University of Southern Mississippi.

‡ Jackson State University.

§ Current address: College of Arts and Sciences, Florida Gulf Coast University, Fort Myers, FL 33965.

(1) Mcmurry, T. J.; Raymond, K. N.; Smith, P. H. *Science* **1989**, *244*, 938.

(2) Weissbuch, I.; Addadi, L.; Lahav, M.; Leiserowitz, L. *Science* **1991**, *253*, 637.

(3) Sessler, J. L.; Lawrence, C. M.; Jayawickramarajah, J. *Chem. Soc. Rev.* **2007**, *36*, 314, and references therein.

(4) Collins, B. E.; Anslyn, E. V. *Chem. Eur. J.* **2007**, *13*, 4700.

(5) Hannon, M. J. *Chem. Soc. Rev.* **2007**, *36*, 280.

(6) Chiari, M.; Cretich, M.; Damin, F.; Carlo, G. D.; Oldani, C. *J. Chromatogr. B* **2008**, *866*, 89, and ref. therein.

(7) Lestage, D. J.; Schleis, D. J.; Urban, M. W. *Langmuir* **2004**, *20*(17), 7027–7035.

(8) Lestage, D. J.; Urban, M. W. *Langmuir* **2005**, *21*, 2150–2157.

(9) Lestage, D. J.; Yu, M.; Urban, M. W. *Biomacromolecules* **2005**, *6*(3), 1561–1572.

(10) Lestage, D. J.; Urban, M. W. *Langmuir* **2005**, *21*, 6753.

(11) Brown, D. A.; London, E. *J. Biol. Chem.* **2000**, *275*, 11722.

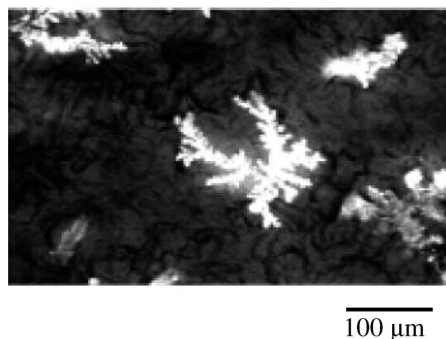(12) Simons, K.; van Meer, G. *Biochem.* **1988**, *27*, 6197.

Figure 1. Cross-polarized optical micrograph of DLPC stabilized p-MMA/nBA film surfaces recorded from the F-A interface.

features of biologically active phospholipids. It turns out that colloidal particle coalescence provides a unique environment for PLs stratification near the F-A and F-S interfaces, which is driven by an access of the surface energy at the interfacial regions, thus often facilitating PL mobility. One of the intriguing phenomena was the ability of PLs to form well organized surface entities referred to as surface localized ionic clusters (SLICs) which form only during particle coalescence and are composed of PLs or a combination of PL and other dispersing agents. Several mechanisms leading to stratification of these species were proposed.[7-10]

Since structural features and interactions of SLICs composed of PLs with polymer surfaces are important for facilitating either attachment or growth of biocomponents to or from polymeric surfaces, this study attempts to determine what structural features are responsible for molecular recognition of PLs and interactions that lead to SLIC formation on poly(methyl methacrylate/*n*-butyl acrylate) (p-MMA/nBA) film surfaces. For that reason synthetic and spectroscopic efforts along with molecular modeling will be employed to advance limited knowledge that may enhance comprehension of lipid−protein recognition and interactions between biological and synthetic systems.

As have been shown in our previous studies, during coalescence of p-MMA/nBA colloidal particles stabilized by biologically active phospholipid dispersing agents SLICs are formed at the F-A and F-S interfaces.[7-10] Figure 1 illustrates an optical image obtained from the F-A of 1,2-dilauroyl-*sn*-glycero-3-phosphocholine (DLPC)-stabilized p-MMA/nBA films and show that crystalline SLIC entities are observed. The F-S interface does not show these features (not shown). For the same copolymer matrix, but prepared in the presence of sodium dioctylsulfosuccinate/1,2-dilauroyl-*sn*-glycero-3-phosphocholine (SDOSS/DLPC), these species are not observed under ambient conditions. If they were formed, their formation would occur only during coalescence of colloidal particles and a number of control experiments in which DLPC and other PLs were solidified from an aqueous phase resulted in the formation of a powdery PL. Thus, the formation of SLICs occurs only in certain areas of coalesced films, thus raising two questions: (1) what chemical entities at the p-MMA/nBA surfaces are responsible for the initiation of SLIC formation and (2) why the presence of colloidal particles facilitates selective SLIC formation.

Experimental Section

Methyl methacrylate (MMA), *n*-butyl acrylate (nBA), sodium dioctylsulfosuccinate (SDOSS), and potassium persulfate (KPS) were purchased from Aldrich Chemical Co. 1,2-Dilauroyl-*sn*-glycero-3-phosphocholine (DLPC) phospholipid was purchased from Avanti Polar Lipids, Inc. p-MMA/nBA copolymer emulsions stabilized by DLPC and SDOSS/DLPC were synthesized, following the procedure
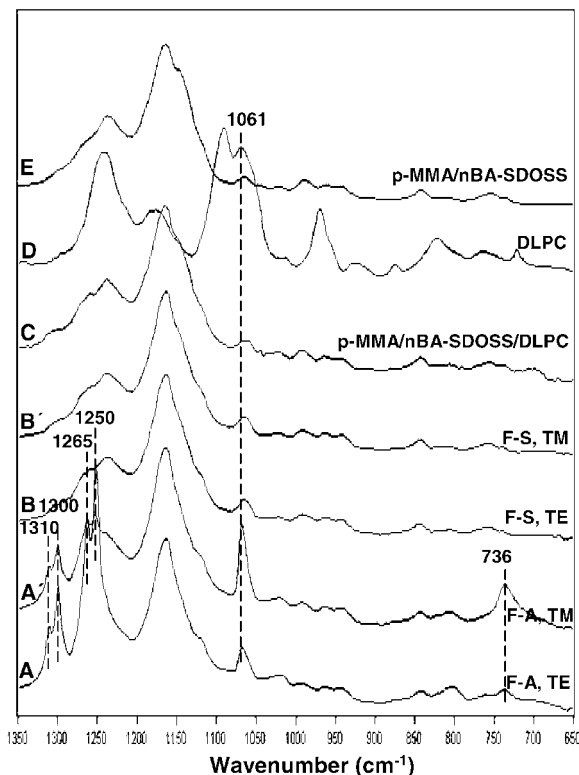

Figure 2. Polarized ATR-FTIR spectra of p-MMA/nBA copolymer films containing DLPC at A, F-A; TE polarization; A′, F-A; TM polarization; B, F-S; TE polarization; B′, F-S; TM polarization; and reference sample: C, p-MMA/nBA copolymer containing SDOSS/DLPC; D, DLPC; and E, p-MMA/nBA copolymer containing SDOSS.

outlined earlier.[9] p-MMA and p-nBA homopolymers containing DLPC were prepared by the same procedure.

The particle size measurements were performed on a Macrotrac Nanotrac 250 instrument. Optical micrographs of film surfaces were obtained using a Nikon Optiphot biological microscope equipped with cross-polarizers. Microscopic attenuated total reflectance Fourier transform infrared (ATR FT-IR) spectroscopic measurements were performed on the film-air (F-A) and film−substrate (F-S) interfaces using a Bio-Rad FTS-6000 FT-IR single-beam spectrometer with 4 cm^{-1} resolution. The surfaces were analyzed using a 2 mm Ge crystal with a 45° angle maintaining constant contact pressure between the crystal and the specimens. All spectra were corrected for spectral distortions using software for the Urban−Huang algorithm.[13] Selected area electron diffraction (SAD) patterns of samples were obtained using a Jeol JEM-2100 transmission electron microscope (TEM) operated at 200 kV.

Computer simulations were carried out in order to determine structural features of SLICs. The choice of theoretical level depends on the accuracy requested and the size of a system. It is well-known that DFT-B3LYP method predicts excellent geometries,[14,15] however, due to the large size of the SLICs systems under consideration, computer simulations at AM1, HF/3-21G, B3LYP[16-19]/6-31G, and B3LYP/6-31G+(d) levels were employed. It has been proven that the HF/3-21G method well reproduces the geometrical parameters. Thus only the models optimized at the HF/3-21G[20-22] level are

(13) Urban, M. W., *Attenuated Total Reflectance Spectroscopy of Polymers-Theory and Practice*; American Chemical Society: Wahsington, DC, 1989.
(14) Bauschlicher, C. W. *Chem. Phys. Lett.* **1995**, *246*, 40.
(15) El-Azhary, A. A.; Suter, H. U. *J. J. Phys. Chem.* **1996**, *100*, 15056.
(16) Becke, A. D. *J. Chem. Phys.* **1993**, *98*, 5648.
(17) Lee, C.; Yang, W.; Parr, R. *Phys. Rev. B* **1988**, *37*, 785.
(18) Miehlich, B.; Savin, A.; Stoll, H.; Preuss, H. *Chem. Phys. Lett.* **1989**, *90*, 5622.
(19) Stephens, P. J.; Devlin, F. J.; Chabalowski, C. F.; Frisch, M. J. *J. Phys. Chem.* **1994**, *98*, 11623.
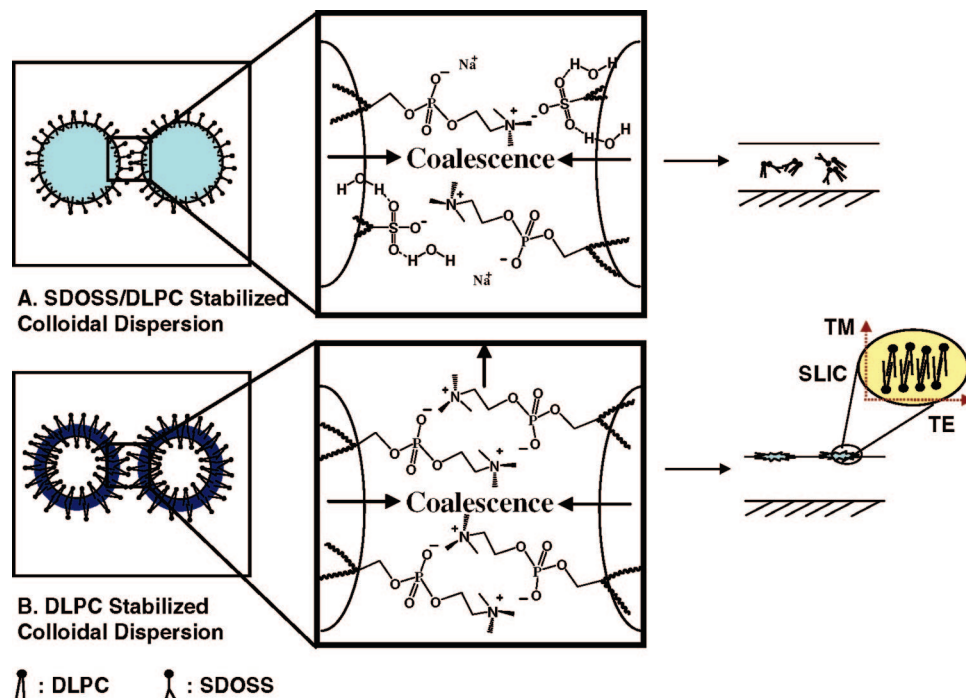
Figure 3. Schematic diagram depicting interactions between DLPC and SDOSS.
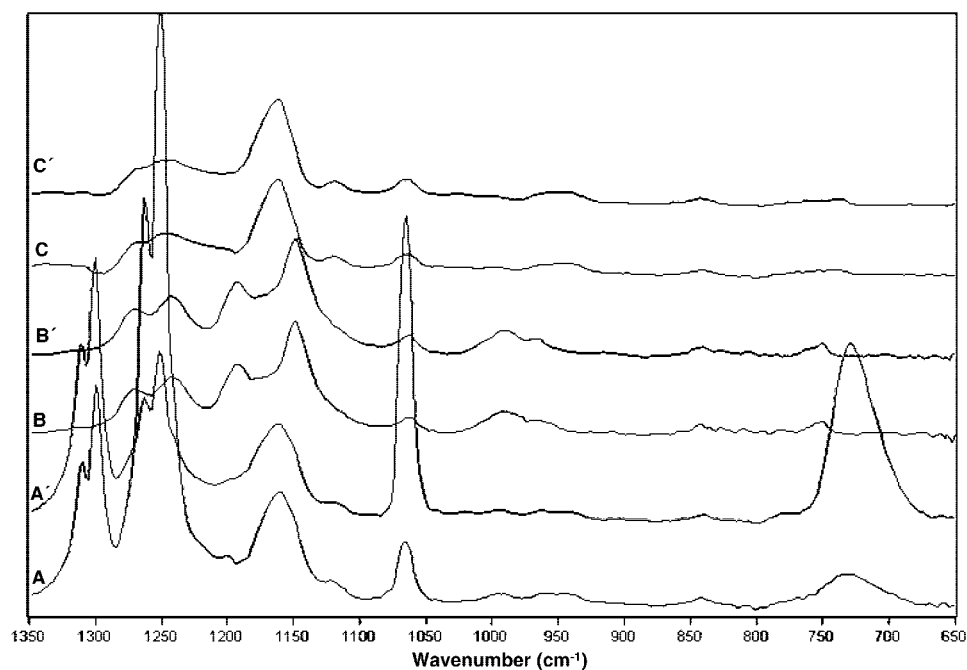

Figure 4. ATR-FTIR spectra of DLPC stabilized p-MMA and p-nBA recorded from the F-A interface: A, p-MMA/p-nBA blend; TE polarization; A′, p-MMA/p-nBA blend; TM polarization; B, p-MMA; TE polarization; B′, p-MMA; TM polarization; C, p-nBA; TE polarization; C′, p-nBA; TM polarization.

discussed in this work unless mentioned otherwise. The characteristics of the local minima were verified by vibration frequency calculations. The harmonic vibrational wavenumbers and absolute intensities were calculated at the same level using the HF/3-21G optimized structures. The values of the wavenumbers were scaled by a factor of 0.964 for HF/3-21G level of theory.[23,24] All calculations were carried out using the Gaussian 03 package.[25]

(20) Roothan, C. C. J. *Rev. Mod. Phys.* **1951**, *23*, 69.
(21) Pople, J. A.; Nesbet, R. K. J. *J. Chem. Phys.* **1954**, *22*, 571.
(22) Dierksen, R. M. G. *J. Chem. Phys.* **1968**, *49*, 4852.
(23) http://cccbdb.nist.gov/vibnotes.asp.
(24) Scott, A. P.; Radom, L. *J. Phys. Chem.* **1996**, *100*, 16502.

Results and Discussion

We utilized ATR FT-IR spectroscopy which allows us to analyze chemical entities at the F-A and F-S interfaces of p-MMA/nBA films. The results of the analysis are illustrated in Figure 2, and Traces A/A′ and B/B′ show spectra recorded from the F-A and F-S interfaces, respectively. The spectra were recorded using TE (Traces A, B) and TM (Traces A′, B′) polarizations in order to determine dichroic ratios of selected bands, and establish preferential spatial orientation of given species responsible for these vibrations. Analysis and comparison of the spectra recorded
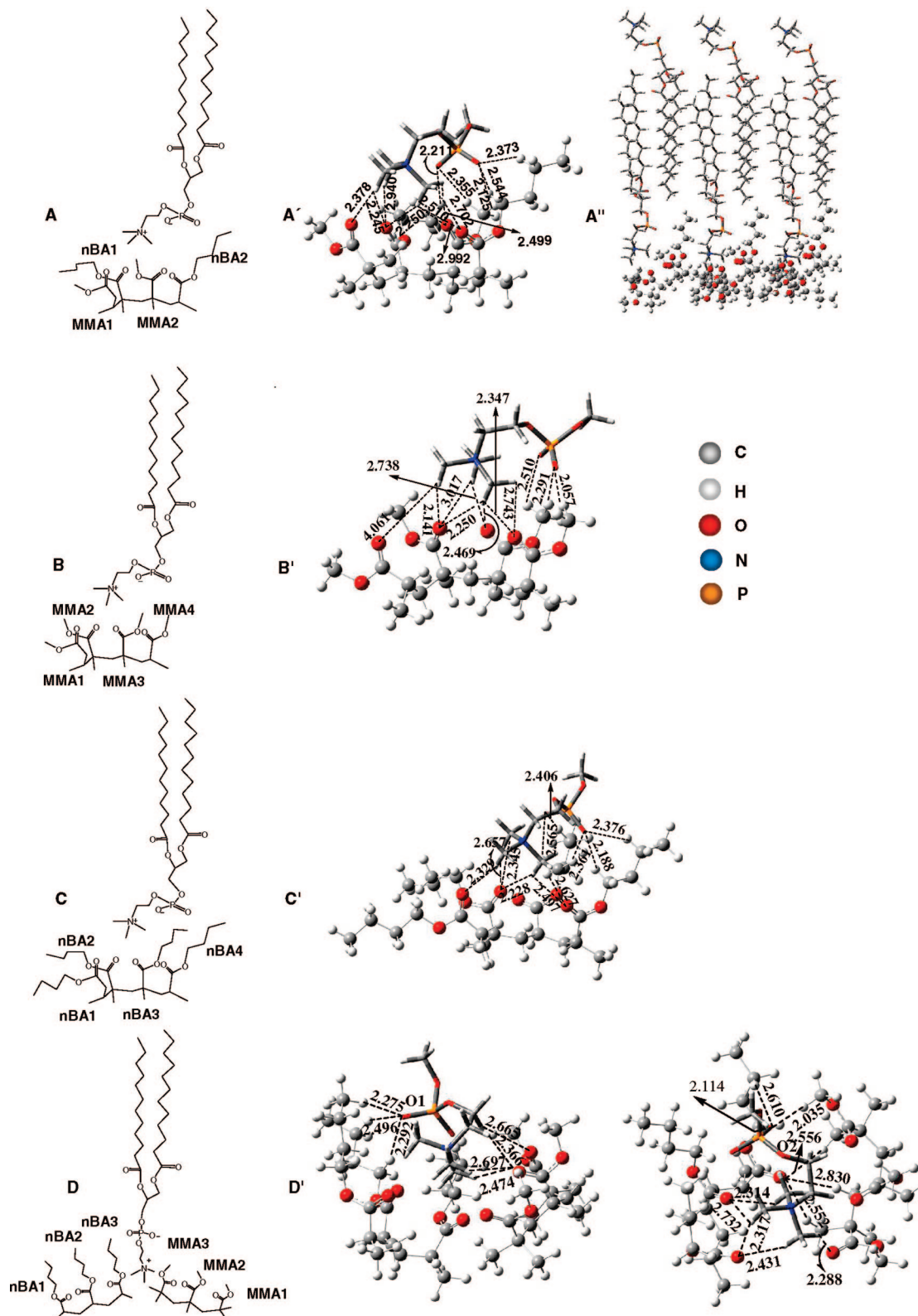
Figure 5. Proposed SLIC models resulting from the interaction between copolymer components and DLPC: A, p-MMA/nBA copolymer; A′, 3D localized p-MMA/nBA copolymer−phospholipid interactions; A″, 3D model of SLICs; B, p-MMA homopolymer; B′, 3D localized p-MMA homopolymer−phospholipid interactions; C, p-nBA homopolymer; C′, 3D localized nBA homopolymer−phospholipid interactions; D, p-MMA/ p-nBA blend; D′, 3D localized p-MMA/p-nBA blend−phospholipid interactions.

from the F-A and F-S interfaces show the presence of the bands at 1310, 1300, 1265, and 1250 cm^{-1} which are not present at the F-S interface. Furthermore, enhanced intensity of the band at 1061 cm^{-1} due to P−O−C segments of DLPC in the TM polarization is observed, with the dichroic ratio of 0.235. The

P−O−C orientation changes originate from the ionic segments of DLPC. These observations indicate preferentially perpendicular orientation of the DLPC head groups with respect to the F-A interface. As shown in Trace C, no IR bands due to SLICs are detected in the films coalesced from the particles stabilized by
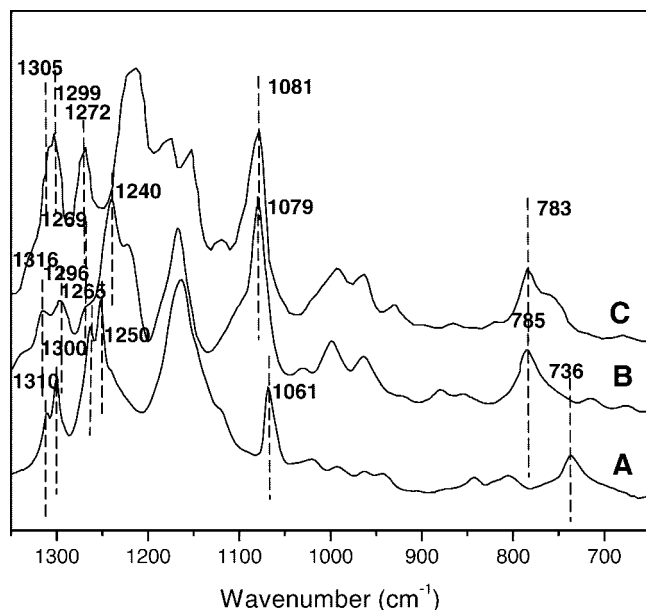
Figure 6. Comparison of (A) combined TE and TM polarized ATR-FTIR spectrum of DLPC stabilized p-MMA/nBA collected from the F-A interface; (B) Calculated IR spectrum from the Model A in Figure 5, (C) Calculated IR spectrum from the Model D in Figure 5.

SDOSS/DLPC.[9] For reference purposes, Traces D and E of Figure 2 illustrate the spectra of DLPC and p-MMA/nBA/SDOSS, respectively, and show virtually no resemblance of the spectra recorded from the F-A and F−S interfaces (Traces A/A′ and B/B′) with the exception of the strong bands at 1148 and 1162 cm^{-1} due to C–O–C of MMA and nBA units.

Before we attempt to address these spectroscopic differences reflecting significant chemical differences, it should be also noted that SDOSS/DLPC stabilized particles exhibit monomodal particle distribution with an average particle size of 132 nm, whereas the same DLPC-stabilized colloidal particles are 69 nm in diameter. These observations indicate that SDOSS/DLPC form larger miscible micelles and form monomodal particles during synthesis. In contrast, previous studies have shown that when hydrogenated soybean phosphatidylcholine (HSPC) and SDOSS are utilized, formation of bimodal particle distribution[7] was observed, which was attributed to dissimilar hydrophobicity and compatibility of HSPC and SDOSS. Furthermore, as shown in Trace C of Figure 2, the presence of SDOSS inhibits DLPC mobility, and thus does not facilitate SLIC formation.[7] This is attributed to ionic interactions between (CH$_3$)$_3$–N$^+$ of DLPC and SO$_3^-$ of SDOSS at the particle interfaces, which inhibit DLPC migration, and is schematically illustrated in Figure 3, A. However, the presence of ionic interactions between (CH$_3$)$_3$–N$^+$ and PO$_4^-$ groups of two DLPC molecules and the hydrophilic nature of phosphocholine groups of DLPC facilitates SLICs formation. As water evaporates, DLPC molecules are released from the particle surfaces and migrate to the F-A interface being forced out of the interfacial regions. This is schematically depicted in Figure 3B. Thus, there is a significant influence of dispersing agents and their interactions with colloidal particles on mobility and stratification during coalescence.

In an effort to establish the influence of the polymer matrix on SLIC formation, ATR FTIR spectra were recorded from the F-A interfaces of DLPC stabilized p-MMA and p-nBA homopolymers, and their blend films. As illustrated in Figure 4, Traces A/A′, ATR FT-IR spectra collected from the F-A interface of a 50:50 p-MMA/p-nBA blend stabilized by DLPC reveal the presence of SLICs, as manifested by the presence of the bands

at 1310, 1300, 1265, 1250, and 1061 cm^{-1} due to SLICs. In contrast, these bands are not detected in Traces B/B′ and C/C′, which represent the spectra recorded from the F-A interface of p-MMA and p-nBA homopolymers containing DLPC. Although these data suggest that the formation of SLICs is attributed to the simultaneous presence of MMA, nBA, and DLPC, further evidence is necessary to determine the origin of their formation and the location of SLICs on the p-MMA/nBA surface.

As indicated above, the formation of SLICs occurs only during particle coalescence, whereas disturbance of the particle surface by other species inhibits or promotes migration to the interfaces, depending upon the nature of chemical interactions. Numerous experimental attempts to recreate SLIC formation outside the colloidal environment resulted in failure, and it became clear that structural features of SLICs are unique, and a prerequisite for their formation is the particle coalescence. Although one could attribute the interfacial surface tension between collating particles generating capillary forces[26] as the main source for mobilizing DLPC to the F-A interface, we believe that this process is an intermediate stage that mobilizes PLs from particle surfaces. The first stage will require the displacement of PLs, such as depicted in Figure 3B, followed by their transport via the capillary forces, and orchestrated alignment of DLPC at the F-A interface. While the first two stages are fairly well documented,[27] and several factors contribute to these efforts, specific interactions that are responsible for the growth of the SLICs shown in Figure 1 in specific locations remain unknown.

In an effort to determine molecular entities responsible for SLIC formation, we calculated IR spectra shown in Figure 2 from molecular modeling experiments. For that purpose we utilized ab initio calculations in which polar ends of DLPC were allowed to interact with p-MMA/nBA copolymer backbone. This approach was stipulated by the experimental data discussed in conjunction with Figures 2 and 4. During simulations, p-MMA and p-nBA homopolymers were allowed to interact independently with DLPC through electrostatic and H-bonding attraction between the anionic phosphate-cationic quaternary ammonium pair and the carbonyls of the copolymer matrices. This choice resulted from ionic interactions detected spectroscopically and shown in Figure 3. Using an ab initio approach, we calculated spectral features responsible for IR bands to match experimentally determined spectra of SLICs shown in Figure 2. Based on the ab initio results that match the experimental data, structural features responsible for SLICs may be deduced.
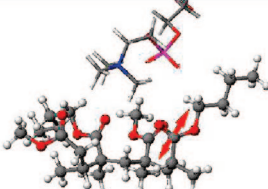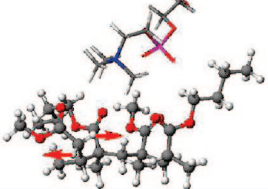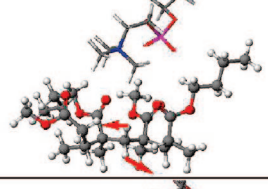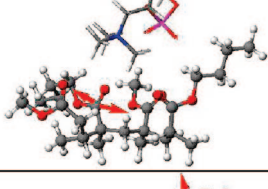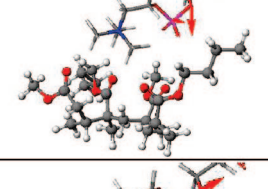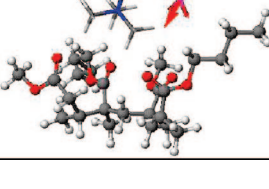
Figure 5A−D illustrates possible interactions derived from the ab initio calculations and show that the most stable configuration is obtained for DLPC-p-MMA/nBA interactions. As seen in Figure 5A, A′, and A″, these interactions occur via DLPC-p-MMA/nBA segments and provide energetically the most stable structure. The distance between the carbonyl O of the

(25) Gaussian 03, Frisch R. R. C., M. J., Trucks, G. W.; Schlegel, H. B.; Scuseria, G. E.; Robb, M. A.; Cheeseman, J. R.; Montgomery, Jr., J. A.; Vreven, T.; Kudin, K. N.; Burant, J. C.; Millam, J. M.; Iyengar, S. S.; Tomasi, J.; Barone, V.; Mennucci, B.; Cossi, M.; Scalmani, G.; Rega, N.; Petersson, G. A.; Nakatsuji, H.; Hada, M.; Ehara, M.; Toyota, K.; Fukuda, R.; Hasegawa, J.; Ishida, M.; Nakajima, T.; Honda, Y.; Kitao, O.; Nakai, H.; Klene, M.; Li, X.; Knox, J. E.; Hratchian, H. P.; Cross, J. B.; Bakken, V.; Adamo, C.; Jaramillo, J.; Gomperts, R.; Stratmann, R. E.; Yazyev, O.; Austin, A. J.; Cammi, R.; Pomelli, C.; Ochterski, J. W.; Ayala, P. Y.; Morokuma, K.; Voth, G. A.; Salvador, P.; Dannenberg, J. J.; Zakrzewski, V. G.; Dapprich, S.; Daniels, A. D.; Strain, M. C.; Farkas, O.; Malick, D. K.; Rabuck, A. D.; Raghavachari, K.; Foresman, J. B.; Ortiz, J. V.; Cui, Q.; Baboul, A. G.; Clifford, S.; Cioslowski, J.; Stefanov, B. B.; Liu, G.; Liashenko, A.; Piskorz, P.; Komaromi, I.; Martin, R. L.; Fox, D. J.; Keith, T.; Al-Laham, M. A.; Peng, C. Y.; Nanayakkara, A.; Challacombe, M.; Gill, P. M. W.; Johnson, B.; Chen, W.; Wong, M. W.; Gonzalez, C.; Pople, J. A. Gaussian, Inc., Wallingford CT, 2004.
(26) Brown, G. L. *J. Polym. Sci.* **1956**, *22*, 423.
(27) Zhao, Y.-Q.; Urban, M. W. *Macromolecules* **2000**, *33*, 7573.

Table 1. Experimental and Calculated IR Bands Obtained from ATR FT-IR Measurements and Ab Initio Calculations Using Models A and D[a]

Experimental IR Band (cm⁻¹)	Calculated IR Band (cm⁻¹)	Vibrational Mode	3D Vibrational Modes
1310	1316 (c) 1305 (b)	C-(C=O) stretching CH vibrational mode	
1300	1296 (c) 1299 (b)	C-(C=O) stretching CH vibrational mode	
1265	1269 (c) 1272 (b)	CH₂ vibrational mode	
1250	1240 (c)	C-(C=O) stretching	
1061	1079 (c) 1081 (b)	P-O-C stretching	
736	785 (c) 783 (b)	P-O stretching	

[a] Note: (c) denotes p-MMA/nBA copolymer; (b) denotes 50:50 p-MMA/p-nBA homopolymer blend.

MMA1 segment and H of the trimethylammonium of DLPC is 2.38 Å, which indicates an existence of strong electrostatic and H-bonding interactions between them. In addition, the short distances between the carbonyl O from the nBA1 and three Hs of the trimethylammonium (2.25, 2.25, 2.94 Å) also stabilize the interaction. Although the MMA2 segment is slightly distorted away from DLPC, there is still an additional weak interaction between the carbonyl O of the MMA2 segment and three Hs of trimethylammonium of DLPC. The distances between the carbonyl O of MMA2 and three Hs of the trimethylammonium are in the range of 2.51−3.32 Å. Similarly, relatively weak interactions between the carbonyl O of nBA2 and the Hs of trimethylammonium on DLPC also stabilize the model A. It should be noted that the PO_2^- segment of DLPC is oriented toward the methyl of MMA and butyl groups of nBA resulting

from attractive forces between the Hs of methyl and butyl groups of the polymer and O^- of PO_2^-. Based on these modeling studies, we conclude that the primary component responsible for SLIC formation results from the presence of neighboring MMA and nBA units and electrostatic attractions between DLPC at the MMA/nBA boundaries. This is illustrated in Figure 5A″.

The same analysis conducted for p-MMA or p-nBA homopolymers at the MMA/MMA or nBA/nBA boundaries with structural features illustrated in Figure 5B−B′ and C−C′ shows that these interactions are not stabilized. As seen in Figure 5B−B′, the model for interactions between p-MMA and DLPC indicates that there are barely any interactions between the MMA1 segment and DLPC as well as the PO_2^- group and MMA1, resulting only from the interaction of methyl groups. In contrast, for p-nBA model illustrated in Figure 5C−C′, the nBA2 unit is fairly
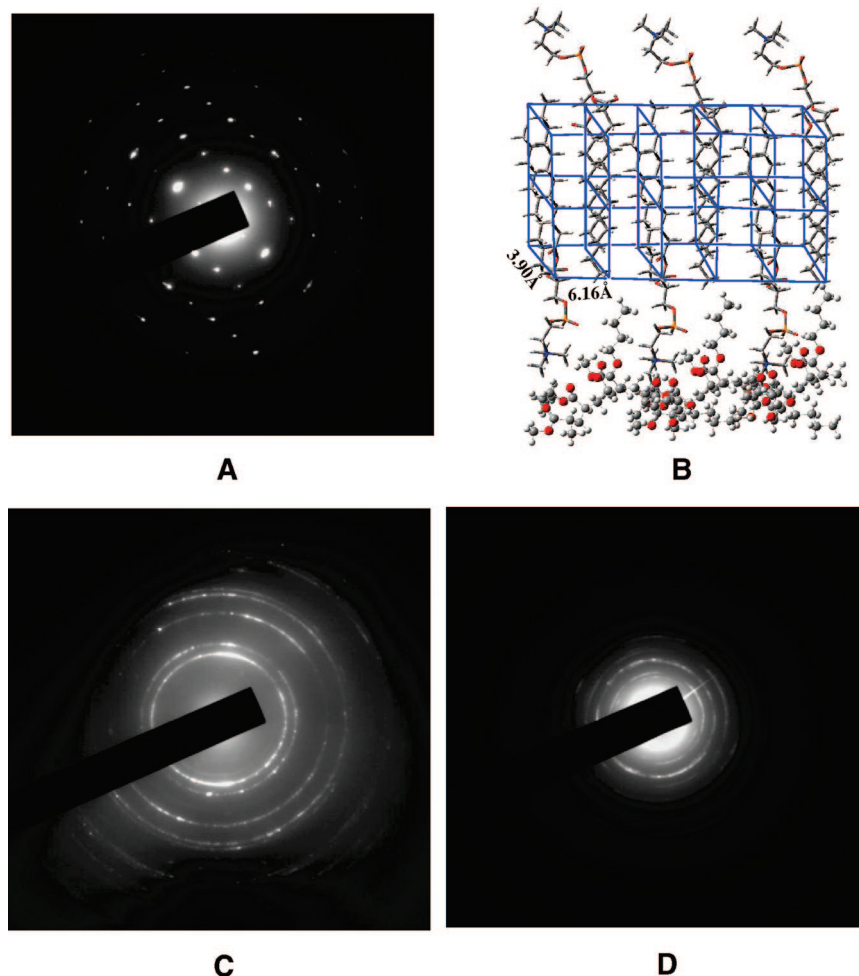
Figure 7. Selected area diffraction images of A, p-MMA/nBA containing DLPC; B, proposed crystal lattice models for SLICs; C, DLPC powder; D, p-MMA/nBA polymer containing SDOSS.

distorted, and the structure is destabilized due to the presence of strong steric repulsions. These features lead to the conclusion that the binding energies of homopolymer structures are significantly less favorable and weaker than those obtained for the copolymer structure with MMA/nBA units.

In order to consider all possible scenarios of potential interactions we determined the feasibility of intermolecular interactions between the neighboring chains of p-MMA and p-nBA homopolymer blends. The results are shown in Figure 5D−D′ which indicate that when a sequence of three MMA and nBA units in the neighboring chains, in the presence of DLPC, also forms SLICs. As seen, when two polymer chains are side-by-side, DLPC forms a bridge between the chains. In this case, H-bonding interactions between the carbonyl oxygen atoms of nBA1 and nBA2, the Hs of trimethyl ammonium of DLPC as well as the carbonyl oxygen atoms of MMA1, MMA2, and MMA3 with DLPC, stabilize the structure. As shown in Figure 5D′, which depicts the side and top views of the structure, the 50:50 p-MMA/p-nBA blend provides a similar environment for the SLIC formation as that observed for p-MMA/nBA copolymer shown in Figure 5A, A′, and A″. Because only three nBA units are involved in the interaction with DLPC on one side, p-nBA chains are less restrained, as that compared with that in p-MMA/nBA copolymer (Figure 5A, A′, and A″), thus providing a more flexible environment for rigid pMMA chains to approach PO_2^- groups. Using ab initio calculations significant H-bonding interactions appear to play an important role in the SLIC formation. Specifically, as shown in Figure 5D−D′, MMA3 group

can approach DLPC closer and H-bonding between the DLPC PO_2^- oxygen O2 atom and the H atoms of nBA3 and the near-neighbor MMA1 are responsible for SLIC formation. Other similar type interactions are also located between the DLPC PO_2^- oxygen O1 atom and the Hs of nBA1 and nBA3 groups which resembles the arm-chair-model structure of the copolymer.

Furthermore, this analysis shows that the existence of the neighboring of MMA and nBA units in the p-MMA/nBA backbone facilitates SLIC formation which is also manifested by a comparison of the experimental and calculated IR spectra. Figure 6, Trace A, illustrates ATR FT-IR spectrum obtained by averaging of the spectra recorded in the TE and TM polarization modes at the F-A interface with the characteristic SLIC bands at 1310, 1300, and 1265, 1250, and 1061 cm^{-1}. For comparison, Trace B of Figure 6 is the calculated IR spectrum obtained from the structure shown in Figure 5A, A′, and A″. Similar results are obtained for the 50:50 p-MMA and p-nBA homopolymer blend. Trace C of Figure 6 illustrates calculated IR spectrum from the structure shown in Figure 5D−D′. Although not all experimental and theoretically predicted IR bands exactly match, the main calculated bands (Trace B) at 1316, 1296, 1269, 1240, 1079, 785 cm^{-1} show good agreement with the experimental results (Trace A). Similarly, for the blend (Trace C) the following bands are obtained: 1305, 1299, 1272, 1081, and 783 cm^{-1}. To illustrate which vibration contributes to specific structural features, characteristic vibrational bands and structural features responsible for these bands are summarized in Table 1. Table 1 also illustrates 3D vibrational modes responsible for the SLIC formation. The

bands at 1310 and 1300 cm^{-1} are attributed to the C—(C=O) stretching and CH vibrational modes, whereas the bands at 1265 and 1250 cm^{-1} result from the CH$_2$ on backbone vibrational modes and C—(C=O) stretching vibrations, respectively. Finally, the band at 1061 cm^{-1} is due to P—O—C stretching, and the band at 736 cm^{-1} is attributed to P—O stretching vibrations.

Although these studies demonstrate for the first time that specificity of PL diester-type polymer interactions is attributed to the presence of MMA and nBA units next to each other, analysis of Figure 1 clearly illustrates the formation of crystallites. In order to determine the size of crystalline lattice of SLICs grown from the p-MMA/nBA surface, SAD was utilized. Figure 7, A, illustrates the single crystal diffraction pattern of the orthorhombic lattice. Using these data we calculated the lattice constants which are 4.0 Å and 6.2 Å. As we recall the results of the ab initio calculations, the distance between DLPC molecules shown in Figure 5A′ gives the crystal lattice constants of 3.90 Å and 6.16 Å, which closely matches the SAD data shown in Figure 7, with the unit cell shown in Figure 7B. For reference, Figure 7C and D, illustrates electron diffraction patterns of DLPC and p-MMA/nBA containing SDOSS, respectively, which do not exhibit single crystal patterns, reinforcing earlier conclusions that the presence of colloidal particles facilitates mobility and transport of DLPC to the surface, while the presence of neighboring MMA and nBA units next to each other facilitates SLIC formation.

Lipid—protein interactions have been studied intensively, but the detailed chemical nature of their interactions is not known. Specifically, questions that need to be address are how membrane proteins interact with the lipids surrounding the membrane proteins or do lipid molecules form shells around a membranes protein. These studies show for the first time that the presence of diester group separated by aliphatic C—C bonds facilitated by covalently bonded methyl methylacrylate and n-butyl acrylate units provides a recognition site for the SLIC formation. These interactions are specific, and occur between C=O and (CH$_3$)$_3$–N$^+$ groups as H-bonding and electrostatic interactions. Although these interactions have been recognized in the protein—lipid studies, their specificity was not identified. After all, p-MMA/nBA copolymer structure and portions of protein structural features exhibit similar hydrophobic groups which may provide environments conducive for amphiphilic lipid crystallization and specific recognition site by PLs.

Conclusions

p-MMA/nBA colloidal dispersions were synthesized in the presence of biologically active phospholipids and upon coalescence lead to the formation of SLICs which are only formed during film formation of colloidal particles. Combination of experimental and theoretical approaches allowed us to determine the nature of the interactions between anionic phosphate groups, cationic quaternary ammonium groups of the phospholipid, and carbonyl groups of the neighboring MMA and nBA units of p-MMA/nBA copolymer. These studies show that the two neighboring MMA and nBA units along the polymer backbone provide conducive environments to signal and attract amphiphilic groups of DLPC, thus initiating SLIC formation. This process is believed to be driven by H-bonding and electrostatic interactions of both units which recognize amphiphatic characteristic species, thus resembling biological recognitions.